Journal of Alloys and Compounds 498 (2010) 203–206

Contents lists available at ScienceDirect

Journal of Alloys and Compounds

journal homepage: www.elsevier.com/locate/jallcom

# Effect of nickel on the electrical properties of nanostructured MnZn ferrite

C. Venkataraju [a,*], G. Sathishkumar [b], K. Sivakumar [c]

[a] Department of Physics, A.M.A. College of Engineering, Vadamavandal, Vellakulam, Kancheepuram 604 401, Tamilnadu, India
[b] Department of Physics, Sri Sairam Engineering College, West Tambaram 600 044, Chennai, India
[c] Department of Physics, Anna University Chennai, Chennai 600 025, India

ARTICLE INFO

*Article history:*
Received 6 October 2009
Received in revised form 17 March 2010
Accepted 19 March 2010
Available online 25 March 2010

*PACS:*
61.10.Nz
61.46.Df
72.20.E
77.84.−S

*Keywords:*
Nanostructured materials
Chemical synthesis
Dielectric response
X-ray diffraction

ABSTRACT

Nano-particles of $Mn_{0.5-x}Ni_xZn_{0.5}Fe_2O_4$ ($x = 0.0$, 0.1, 0.2, 0.3 and 0.5) have been synthesized by chemical co-precipitation method. The lattice constant (Å) for all Mn/Ni concentration is found to be less than that for the corresponding bulk values. The X-ray intensity of the (4 4 0) plane increases with increasing $Ni^{2+}$ concentration indicating the occupation of $Ni^{2+}$ ions on octahedral sites. The dielectric constant decreases with the increase in Ni concentration except for $x = 0.3$. Relaxation peaks were observed for all the samples in tan $\delta$ versus frequency curves and the relaxation peaks shift towards lower frequency for higher nickel concentration. The resistivity was found to increase with increase in Ni concentration and decreases with increase in temperature.

## 1. Introduction

Manganese zinc ferrites are technologically important because of their permeability and high magnetization. However their eddy current loss is higher at higher frequencies because of their low resistivity. These ferrites have been widely used in electronic applications such as transformers, coils, recording heads, etc. Nickel–zinc ferrite on the other hand possesses high resistivity but relatively low permeability at high frequencies. This ferrite has been extensively used as a magnetic core material for a large number of devices and electrical components such as phase shifters, circulators, isolators, inductors and transformers. Properties of these ferrites have been investigated separately but few reports are available on the combination of these two ferrites. Verma et al. [1] have reported the development of a new power ferrite with low power loss based on manganese–nickel–zinc ferrite composition for switched mode power supplies. Singh et al. [2] have reported the effect of cation distribution on the properties of $Mn_{0.2}Ni_{0.8x}Zn_xFe_2O_4$. High frequency magnetic applications require ferrites with high permeability and high resistivity. In the present investigation the influence of $Ni^{2+}$ ions in manganese–nickel–zinc ferrite on the densification, lattice constant, dielectric constant and electrical resistivity is examined in order to utilize the best of properties of the two ferrites.

## 2. Experimental details

Nano-particles of $Mn_{(0.5-x)}Ni_xZn_{0.5}Fe_2O_4$ (with $x = 0.0$, 0.1, 0.2, 0.3 and 0.5) were prepared by co-precipitation method. Aqueous solutions of $MnCl_2$, $ZnSO_4$, $NiCl_2$ and $FeCl_3$ in their respective stoichiometry (100 ml of solution containing $(0.5 - x)$ M $MnCl_2$, $(x)$ M $NiCl_2$, 0.5 M $ZnSO_4$ and 100 ml of 2 M $FeCl_3$) were mixed thoroughly at 80 °C and this mixture was added to the boiling solution of NaOH (0.55 M dissolved in 1600 ml of distilled water) within 10 s under constant stirring and a pH of 11 was maintained throughout the reaction. Conversion of metal salts into hydroxides and subsequent transformation of metal hydroxide into nano-ferrites takes place upon heating to 100 °C and maintained for 60 min. The nano-particles thus formed were isolated by centrifugation and washed several times with deionized water followed by acetone and then dried at room temperature. The dried powders were mixed with an organic binder (polyvinyl alcohol) 2 wt%, and pressed into pellets of 10 mm diameter by applying a pressure of 5 ton. The samples are sintered in air for 5 h at 500 °C. The electrical contacts were made by coating silver paint on the flat surfaces of the sintered pellets. The dielectric constant was calculated from capacitance measurements made on a HIOKI 3532-50 LCR HiTester as a function of frequency from 1 kHz to 5 MHz. The corresponding loss tangent tan $\delta$ was also measured. The data collection was performed on a PAN analytical expert PRO X-ray diffractometer using Cu K$\alpha$ radiation. Data were collected every 0.02° in the angle range 20–70° in $2\theta$. The particle size was determined by subjecting the samples to transmission electron microscopy (TEM) using a Philips CM20 microscope. Resistivity as a function of temperature was measured by using two-probe method.

---

* Corresponding author. Tel.: +91 4182 247226; fax: +91 4182 247518.
*E-mail address:* cvraju_2k@yahoo.com (C. Venkataraju).

0925-8388/$ – see front matter © 2010 Elsevier B.V. All rights reserved.
doi:10.1016/j.jallcom.2010.03.160

## 3. Results and discussion

### 3.1. XRD analysis

The X-ray diffraction pattern for $Mn_{(0.5-x)}Ni_xZn_{0.5}Fe_2O_4$ (with $x = 0.0$, 0.1, 0.2, 0.3 and 0.5) is shown in Fig. 1. These diffraction lines provide clear evidence of the formation of ferrite phase in all the samples. The broad XRD line indicates that the ferrite particles are of nano-size. The average particle size for each composition was calculated from the XRD line width of the (3 1 1) peak using Scherrer formula [3]. The values of the particle size and lattice constant as deduced from the X-ray data are given in Table 1. The average particle size for $Mn_{0.4}Ni_{0.1}Zn_{0.5}Fe_2O_4$ was found to be 19 nm. The lattice constant decreases with increasing nickel concentration up to $x = 0.2$, which can be explained based on the relative ionic radius. The ionic radius (0.69 Å) of $Ni^{2+}$ ions is smaller than the ionic radius (0.82 Å) of $Mn^{2+}$ ions. Hence replacement of smaller $Ni^{2+}$ cations for larger $Mn^{2+}$ cations in the manganese zinc ferrite causes a decrease in lattice constant. However the lattice constant of the samples was found to be less than that of bulk. The bulk value of lattice constant for $Mn_{0.5}Zn_{0.5}$ ferrite reported in the literature by other method is 8.480 Å [4] as compared to the values observed in the present investigation. The low value of lattice constant may also be attributed to a significant fraction of $Mn^{2+}$ and $Zn^{2+}$ occupying the octahedral sites and forcing $Fe^{3+}$ to the tetrahedral sites against their chemical preferences. Since $Fe^{3+}$ ions have smaller ionic radius (0.64 Å), occupying the tetrahedral sites in place of larger divalent ions leads to contraction in lattice parameter of nanostructured ferrite as observed. It is observed that there is an increase in the lattice constant of the sample $x = 0.3$. This is due to the possible presence of the $Fe^{2+}$ ions on the octahedral sites. Since the ionic radius (0.74 Å) of $Fe^{2+}$ ions is greater than the ionic radius (0.64 Å) of $Fe^{3+}$, there is an increase in the lattice constant of the sample $x = 0.3$. The lattice constant for nano-sized $Ni_{0.5}Zn_{0.5}$ ferrite obtained in the present investigation is slightly higher than the corresponding bulk value of 8.399 Å [5]. A similar observation was also reported by Upadhyay et al. [6] for the samples in the nanometer range. The enhancement in the lattice constant is attributed to the interface structure with a large volume fraction [7]. The intensities of the (2 2 0) and (4 4 0) planes are more sensitive to cations on tetrahedral and octahedral sites respectively [8,9]. $Ni^{2+}$ ion has preference for octahedral sites while $Mn^{2+}$ and $Fe^{3+}$ ions have preference for both tetrahedral and octahedral sites respectively [10–12]. Table 2 shows the intensity of the above two planes. The intensity of the (4 4 0) plane increases with increasing $Ni^{2+}$ concentration. This is due to occupation of $Ni^{2+}$ ions on octahedral sites. This results in the migration of $Fe^{3+}$ ions from B site to A site in place of $Mn^{2+}$ ions. Therefore there is also a small increase in the intensity of the (2 2 0) plane up to $x = 0.2$. Due to the formation of $Fe^{2+}$ ions on octahedral sites for sample $x = 0.3$, the migration of $Fe^{3+}$ ions from octahedral sites to tetrahedral sites decreases and hence decreasing the intensities of (2 2 0) plane.

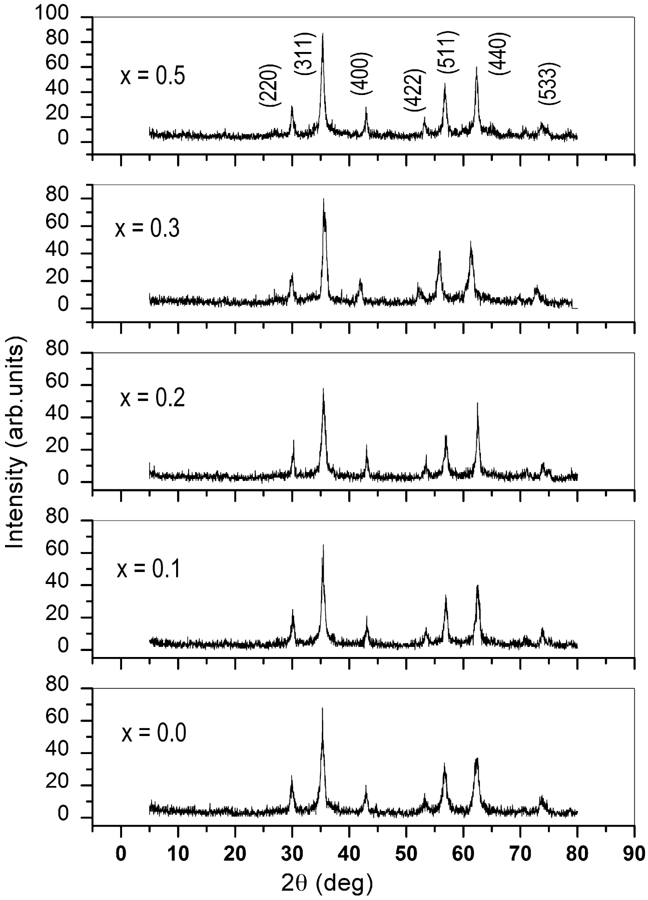

**Fig. 1.** XRD pattern for the system $Mn_{(0.5-x)}Ni_xZn_{0.5}Fe_2O_4$ ($x = 0.0$, 0.1, 0.2, 0.3 and 0.5).

**Table 1**
Lattice constant and particle size of the prepared samples.

| S. no. | Composition | Lattice constant (Å) | Particle size (nm) |
|---|---|---|---|
| 1. | $Mn_{0.5}Zn_{0.5}Fe_2O_4$ | 8.425 | 18 |
| 2. | $Mn_{0.4}Ni_{0.1}Zn_{0.5}Fe_2O_4$ | 8.392 | 19 |
| 3. | $Mn_{0.3}Ni_{0.2}Zn_{0.5}Fe_2O_4$ | 8.375 | 18 |
| 4. | $Mn_{0.2}Ni_{0.3}Zn_{0.5}Fe_2O_4$ | 8.404 | 17 |
| 5. | $Ni_{0.5}Zn_{0.5}Fe_2O_4$ | 8.411 | 23 |

**Table 2**
Observed intensity data.

| S. no. | Composition | I (2 2 0) | I (4 4 0) |
|---|---|---|---|
| 1. | $Mn_{0.5}Zn_{0.5}Fe_2O_4$ | 23.15 | 56.31 |
| 2. | $Mn_{0.4}Ni_{0.1}Zn_{0.5}Fe_2O_4$ | 25.46 | 66.31 |
| 3. | $Mn_{0.3}Ni_{0.2}Zn_{0.5}Fe_2O_4$ | 31.46 | 70.70 |
| 4. | $Mn_{0.2}Ni_{0.3}Zn_{0.5}Fe_2O_4$ | 24.04 | 56.32 |
| 5. | $Ni_{0.5}Zn_{0.5}Fe_2O_4$ | 27.12 | 58.43 |

### 3.2. Transmission electron microscopy analysis

The particle size and morphology of the sample with $x = 0.1$ are shown in Fig. 2. The average particle size is around 22 nm. TEM analysis revealed that the particles are nearly spherical and are non-agglomerated.

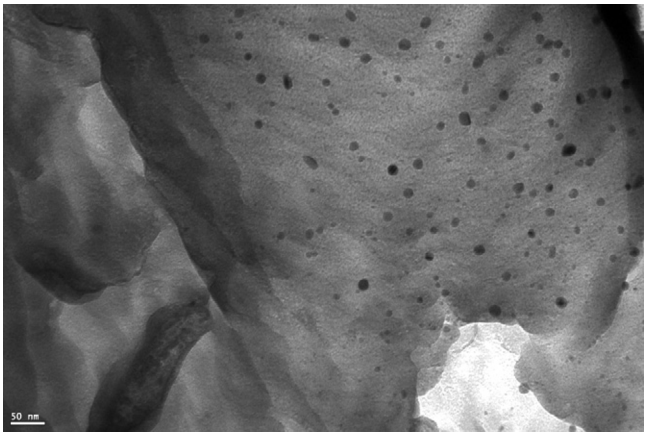

**Fig. 2.** TEM images of $Mn_{0.4}Ni_{0.1}Zn_{0.5}Fe_2O_4$.

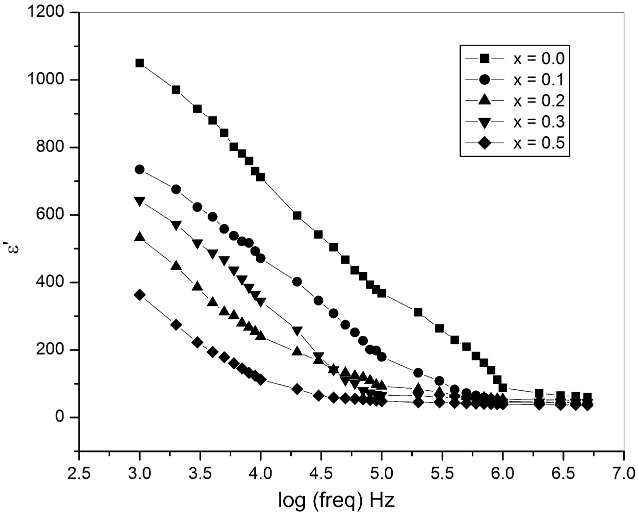

**Fig. 3.** Dielectric constant for the system $Mn_{(0.5-x)}Ni_xZn_{0.5}Fe_2O_4$ ($x = 0.0, 0.1, 0.2, 0.3$ and $0.5$).

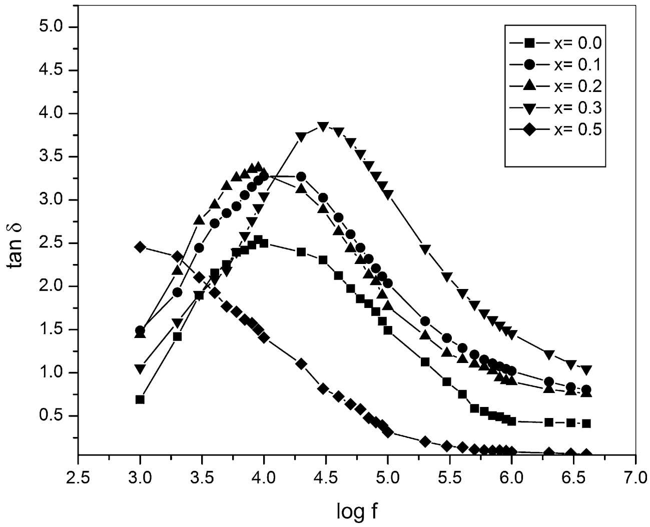

**Fig. 4.** Dielectric loss for the system $Mn_{(0.5-x)}Ni_xZn_{0.5}Fe_2O_4$ ($x = 0.0, 0.1, 0.2, 0.3$ and $0.5$).

### 3.3. *Dielectric studies*

The effect of frequency ($\omega$) on the dielectric constant ($\varepsilon'$) at 300 K for samples with $x = 0.0$–$0.3$ and $x = 0.5$ is illustrated in Fig. 3. The dielectric constant for all the samples is lower than the corresponding bulk value at room temperature. Latha et al. [13] have reported a dielectric constant of $(17–32) \times 10^5$ at 308 K measured at a frequency of 5 kHz for Mn–Zn ferrite in bulk form synthesized by ceramic method. In the present investigation a dielectric constant of 840 is obtained, which is measured at a frequency of 5 kHz at 300 K. This low value of dielectric constant is attributed to homogeneity, better symmetry, uniform and smaller grains [14]. Smaller grains contain large surface boundaries and are the regions of high resistance. This reduces the interfacial polarization and hence the dielectric constant is found to be three orders lesser than that reported for bulk materials. It can be seen from Fig. 3 that the value of the dielectric constant decreases with increasing frequency and the dispersion of dielectric constant is maximum for $Mn_{0.5}Zn_{0.5}Fe_2O_4$. This can be explained on the basis of space charge polarization model of Wagner [15] and Maxwell [16] and is also in agreement with the Koop's phenomenological theory [17]. The decrease of dielectric constant at higher frequency can be explained on the basis that the solid is assumed as composed of well conducting grains separated by poorly conducting grain boundaries. The electrons reach the grain boundary through hopping and if the resistance of the grain boundary is high enough, electrons pile up at the grain boundaries and produce polarization. However, as the frequency of the applied field is increased beyond a certain value, the electrons cannot follow the alternating field. This decreases the probability of electrons reaching the grain boundary and as a result polarization decreases [16,17]. The compositional dependence of dielectric constant is observed to decrease with increase in nickel concentration except for sample $x = 0.3$ where it shows a rise. When $Ni^{2+}$ is substituted for $Mn^{2+}$, it occupies the octahedral B sites. Due to this some of the $Fe^{3+}$ ions migrate from the octahedral B sites to tetrahedral A sites. Therefore the hopping between $Fe^{2+}$ and $Fe^{3+}$ ions decreases in the octahedral sites. As a result, the polarization and hence, the dielectric constant decreases for samples up to $x = 0.2$. This behavior has not been observed for sample $x = 0.3$. This is due to formation of $Fe^{2+}$ ions on the octahedral sites giving rise to electron hopping between the $Fe^{2+}$ ions and $Fe^{3+}$ ions. Therefore polarization increases and hence the dielectric constant increases.

The variation of dielectric loss factor ($\tan\delta$) and imaginary part of dielectric constant ($\varepsilon''$) is shown in Figs. 4 and 5 respectively. It is observed that the loss tangent and imaginary part of dielectric constant decrease initially with increasing frequency followed by the appearance of the relaxation peak.

The appearance of relaxation peak can be explained according to the Debye relaxation theory [18]. The loss peak occurs when the applied field is in phase with the dielectrics and the condition $\omega\tau = 1$ is satisfied, where $\omega = 2\pi f$, f being the frequency of the applied field. Singh et al. [19] have observed a similar relaxation peak at a frequency of 1 kHz for Mn substituted Ni–Zn ferrites synthesized by the citrate precursor method. In the present investigation, the relaxation peak for all the samples appears between the frequencies 1 kHz and 10 kHz. The shifting of the relaxation peak towards lower frequency side with an increase in nickel content ($x$) is due to the strengthening of the dipole–dipole interactions causing hindrance to the rotation of the dipoles [19]. Therefore the resonance between rotation of the dipoles and applied field takes place at lower frequency.

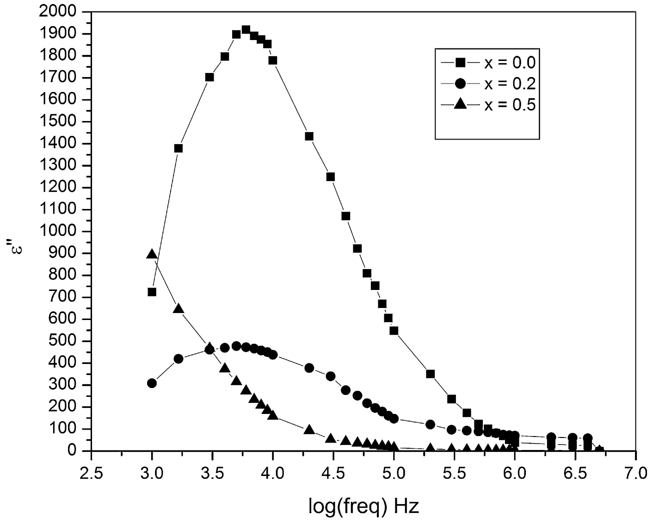

**Fig. 5.** Variation of imaginary part of dielectric constant $\varepsilon''$ with log frequency at room temperature.

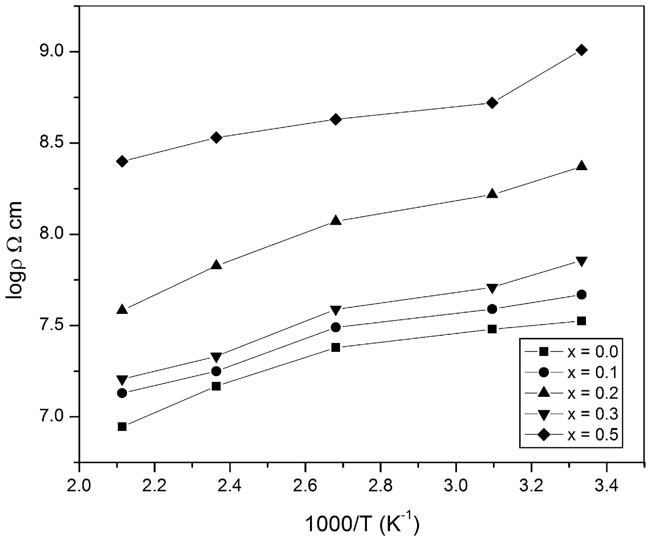

**Fig. 6.** dc resistivity for the system $Mn_{(0.5-x)}Ni_xZn_{0.5}Fe_2O_4$ ($x = 0.0$, 0.1, 0.2, 0.3 and 0.5).

### 3.4. *dc resistivity*

Compositional variation of dc resistivity for different temperatures is shown in Fig. 6. It is observed that the resistivity increases for increase in nickel content. According to Verwey's [20] hopping mechanism, the electrical conduction in ferrites results from a hopping of the electrons between the ions of the same element, but of different valence states present at the octahedral or B site. It is known that zinc and nickel ions occupy tetrahedral (A sites) and octahedral (B sites) positions respectively. While iron and manganese ions occupy both A sites and B sites. In some cases Zn occupies octahedral sites. When $Ni^{2+}$ ions are introduced at the cost of $Mn^{2+}$, some of the iron ions migrate from B sites to A sites, decreasing thereby the $Fe^{3+}$ ion concentration at the octahedral (B sites). Also $Ni^{2+}$ ions are not so easily oxidized to $Ni^{3+}$ and hence the resistivity increases. The change in the cation distribution in the nano-crystalline Mn–Ni–Zn ferrite may also contribute to the observed increase in resistivity. $Zn^{2+}$ ions strongly prefer tetrahedral sites but in the nano-crystalline Mn–Ni–Zn ferrite there is a partial transfer of $Zn^{2+}$ ions from A site to B site The presence of $Zn^{2+}$ ions in the octahedral sites (B sites) blocks the Verwey's hopping mechanism, resulting in an increase in dc resistivity. The dc resistivity obtained in the present investigation is higher than the reported value of bulk counterpart [21]. Singh et al. [22] have reported values of dc resistivity between $1.4 \times 10^5$ Ω cm and $7.3 \times 10^7$ Ω cm for $Ni_xMn_{0.4-x}Zn_{0.6}Fe_2O_4$ (with $x = 0.1$–0.4) synthesized by citrate precursor method. In the present investigation the measured value of dc resistivity for all the samples lies in the range $3.4 \times 10^7$ Ω cm to $1.02 \times 10^9$ Ω cm. This higher value of resistivity is attributed to small grain size. Smaller grains contain a large number of grain boundaries, which act as scattering centers for the flow of electrons and therefore increases the resistivity. It is also observed that the dc resistivity decreases with increasing temperature indicating the semiconducting nature of the samples. This is due to the increase in drift mobility of the charge carriers.

## 4. Conclusion

Nano-sized Mn–Ni–Zn ferrites were prepared by co-precipitation method. The values of dielectric constant and loss factor are significantly lower as compared to those reported for bulk ferrite. The dielectric constant decreases with increase in Ni concentration except for the sample $x = 0.3$. Relaxation peaks were observed for all the samples in tan $\delta$ versus frequency curves. The resistivity was found to increase with increase in nickel concentration and decreases with increase in temperature.

## References

[1] A. Verma, M.I. Alam, R. Chatterjee, T.C. Goel, R.G. Mendiratta, J. Magn. Magn. Mater. 300 (2006) 500–505.
[2] A.K. Singh, A. Verma, O.P. Thakur, C. Prakash, T.C. Goel, R.G. Mendiratta, Solid State Commun. 125 (2003) 121–125.
[3] B.D. Cullity, Elements of X-Ray Diffraction, Addison–Wesley Pub. Co. Inc., 1978, p. 102.
[4] A.H. Morrish, P.E. Clark, Phys. Rev. B 11 (1975) 278.
[5] L.K. Leung, B.J. Evans, A.H. Morrish, Phys. Rev. B 8 (1973) 29.
[6] C. Upadhyay, Verma, S. Anand, J. Appl. Phys. 95 (2004) 5746.
[7] H. Gleiter, Prog. Mater. Sci. 33 (1989) 223.
[8] B.P. Ladgaonkar, A.S. Vaingainkar, Mater. Chem. Phys. 56 (1998) 280.
[9] C.S. Narasimhan, C.S. Swamy, Physica Status Solidi (a) 59 (1980) 817.
[10] K.H. Rao, S.B. Raju, R.G. Gupta, R.G. Mendiratta, Solid State Commun. 36 (1980) 777.
[11] J. Smit, H.P.J. Wijn, Ferrites, Philips Technical Library, Eindhoven, The Netherlands, 1959, p. 149.
[12] R.G. Gupta, R.G. Mandiratta, J. Appl. Phys. 48 (1977) 2998.
[13] K. Latha, K. Sathya Mohan, D. Ravinder, Physica Status Solidi (a) 142 (1994) K103.
[14] P. Mathur, A. Thakur, M. Singh, Phys. Scr. 77 (2008), 045701 (6 pp.).
[15] K.W. Wagner, Am. Phys. 40 (1973) 817.
[16] J.C. Maxwell, Electricity and Magnetism, vol. 1, Oxford University Press, New York, 1973, p. 828.
[17] C.G. Koops, Phys. Rev. 83 (1951) 121.
[18] U.N. Trivedi, M.C. Chhantbar, K.B. Modi, H.H. Johi, Indian J. Pure Appl. Phys. 43 (2005) 688–690.
[19] A.K. Singh, T.C. Goel, R.G. Mendiratta, J. Appl. Phys. 91 (2002) 6626.
[20] J.W. Verwey, J.H. de Boer, Rec. Trav. Chim. Phys-Bas. 55 (1936) 531.
[21] J. Smit, H.P.J. Wijn, Ferrites, Philips Technical Library, Eindhoven, The Netherlands, 1959, p. 234.
[22] A.K. Singh, A.K. Singh, T.S. Goel, R.G. Mendiratta, J. Magn. Magn. Mater. 281 (2004) 276–280.